Circulating Current Control in MMC Under the Unbalanced Voltage

Ji-Woo Moon, *Student Member, IEEE*, Chun-Sung Kim, *Student Member, IEEE*, Jung-Woo Park, Dae-Wook Kang, *Member, IEEE*, and Jang-Mok Kim, *Member, IEEE*

Abstract—This paper proposes a control method for circulating currents in modular multilevel converters (MMCs) under unbalanced voltage conditions. Under balanced voltage conditions, only negative-sequence circulating currents exist. Consequently, the conventional method has considered only negative-sequence circulating currents in MMC. However, under unbalanced voltage conditions, there are positive-sequence circulating currents, zero-sequence circulating currents, and negative-sequence circulating currents in MMC. Thus, under unbalanced voltage conditions, a control method should consider all of these components. This study adopts a dual vector current controller as an ac-side current controller to reduce the ac-side active power ripple under unbalanced voltage. It analyzes the effect of the unbalanced voltage on circulating currents in MMC and then proposes a control method considering each component of circulating currents under the unbalanced voltage. The effectiveness of the proposed controlling method is verified through simulation results using PSCAD/EMTDC.

Index Terms—Circulating current, dual vector current control (DVCC), modular multilevel converter (MMC), negative sequence, positive sequence, zero sequence.

I. INTRODUCTION

CURRENTLY, the number of investments and studies have increased for high-voltage direct-current (HVDC) transmission systems to enhance the efficiency and reliability of ac networks, which have applications for high-capacity electric power transmission and provide links between different power grids, such as China's large-scale HVDC Investment Plan, the European Super Grid, and North America's 2030 Project.

HVDC systems can be divided into two converter types: current-source converter HVDC (CSC-HVDC) and voltage-source converter HVDC (VSC-HVDC). The interest in VSC-HVDC systems is increasing because of the need for active control for renewable energy systems and stabilization for electrical power systems [1], [2]. Compared to CSC-HVDC, VSC-HVDC has the advantages of being able to control active power and reactive power independently, reduce the size of grid-side ac filters, and improve the transient response characteristics by using the PWM method. This system also has no need for a transformer to assist in the commutation process [3].

The multilevel converters applied to VSC–HVDC are divided into three types: 1) diode-clamped multilevel converter (DCMC), 2) flying capacitor multilevel converter (FCMC), and 3) modular multilevel converter (MMC). Among them, DCMC and FCMC have been applied to a limited extent because of the difficulty in modularization and the need for additional clamping diodes and flying capacitors [4]. In contrast, MMCs have the merits of extendibility to hundreds of voltage levels because of their simple circuit structure and easy modularization despite the need for a reactor to suppress the circulating current. Consequently, MMCs are the most suitable structures for obtaining high dc voltage, and many studies have been carried out on them [5]–[15].

MMCs were first proposed in [16]. Fig. 1 shows the structure of a three-phase MMC with six arms. Each arm is composed of a series of connected half-bridge submodules (SMs). An MMC possesses a voltage difference between a dc link and each arm with SMs, which leads to a problem of circulating currents in each arm. References [17] and [18] analyzed the amplitude of circulating currents according to the arm inductance and the SM's capacitance. As the arm inductance increases, the amplitude of the circulating currents decreases. However, despite the increase in arm inductance, circulating currents are not reduced completely, which is inefficient in terms of the cost-benefit analysis. Thus, a control method for circulating currents is necessary.

Reference [19] proposed a method of controlling an MMC's circulating currents. Under the balanced voltage condition, the negative-sequence component of circulating currents in each arm rotates at the double-line frequency. Therefore, a control method was proposed that controlled circulating currents in each arm frame by transforming an a-c-b sequence with a double line-frequency into a d–q sequence at the rotational reference frame. However, this method has the disadvantage of not being able to completely reduce circulating currents under unbalanced voltage conditions, because circulating currents
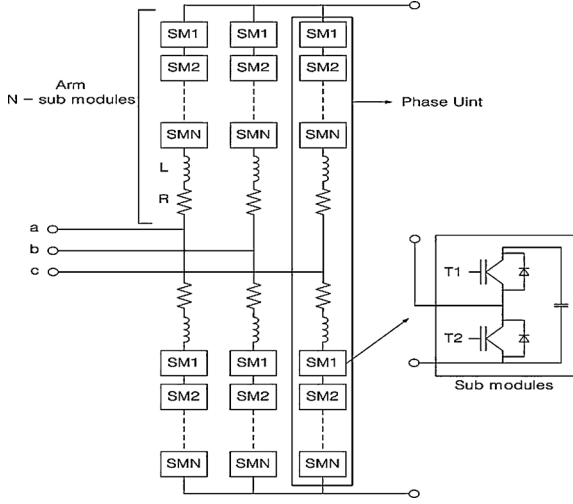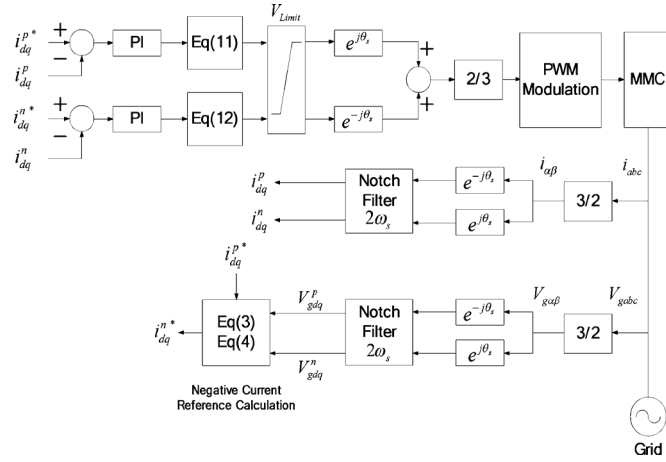
Fig. 1.   Basic structure of MMC.

Fig. 2.   Positive-sequence and negative-sequence inner current controller.

Fig. 3.   Single-phase equivalent circuit of the three-phase MMC.
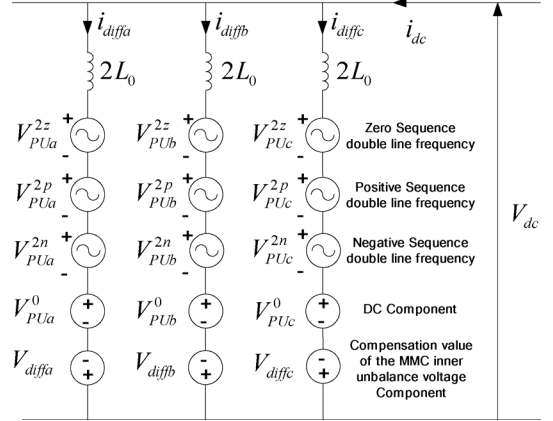
Fig. 4.   Generalized equivalent circuit diagram of the MMC under unbalanced conditions.
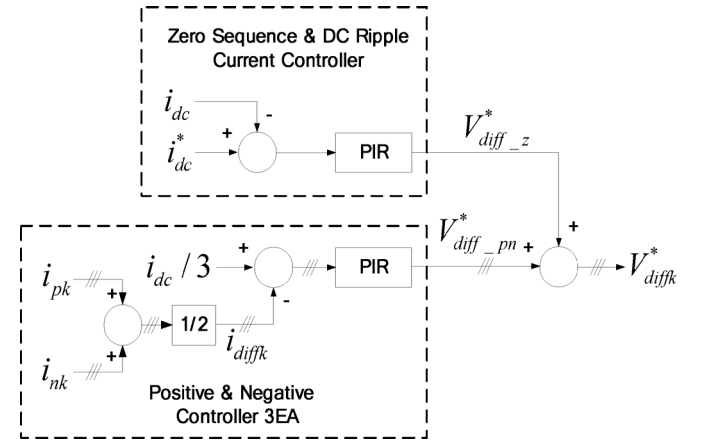
Fig. 5.   Proposed circulating currents control scheme.

have also positive-sequence components and zero-sequence components besides negative-sequence components.

Reference [2] proposed a control method for MMC under unbalanced voltage conditions. It analyzed the instantaneous power of each arm under unbalanced voltage conditions and proposed a control algorithm for reducing circulating currents and dc-link voltage ripples. However, this algorithm has the disadvantage of the inclusion of a double-line-frequency ripple in ac-side active power by controlling ac-side negative-sequence currents to zero under unbalanced voltage conditions.

Reference [20] proposed a control method for circulating currents in an a-b-c stationary frame. Since circulating currents have positive-, negative-, and zero-sequence components under unbalanced voltage conditions, a control method for circulating currents was proposed by considering these components. However, this method has the disadvantage of generating a phase delay because of its utilization of a high-pass filter to separate circulating currents; further, it cannot improve the transient response occurring in the inner unbalanced currents and dc-link currents under unbalanced voltage conditions.

Reference [6] proposed an MMC control method using model predictive control (MPC). The authors organized the cost function to control ac-side currents, circulating currents, and SM voltage balancing using the MPC method and detected the switch status to minimize the cost function. However, this method has a disadvantage in the calculation volume of the processor, which increases with an increase in the level of the MMC because it should decide the switching status with C_{2N}^{N} when the MMC is at the $N + 1$ level.

This study analyzed each phase's instantaneous power to reduce the MMC's ac-side active power ripple when the negative-sequence component was generated under unbalanced voltage conditions. The instantaneous power begins to have
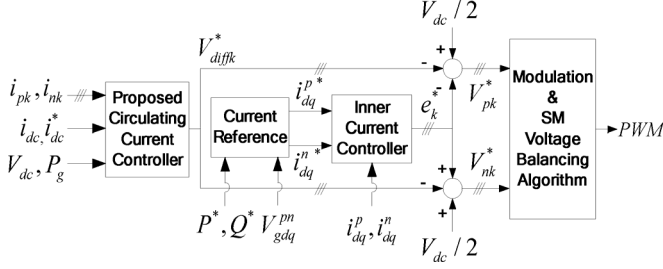
Fig. 6. Control scheme of the MMC, including proposed circulating current control.

Fig. 7. System structure of simulations.

TABLE I
MAIN CIRCUIT PARAMETERS

Items	Values
Active Power	4MW
Reactive Power	0.8MVar
AC System Voltage	11500V
AC System Inductance	19.35mH
DC Bus Voltage	20kV
DC Resistance	0.1ohm
Number of SMs per arm	10
SM Capacitance	0.002F
SM Capacitor Voltage	2000V
Arm Inductance	0.03H
Carrier Frequency	500Hz

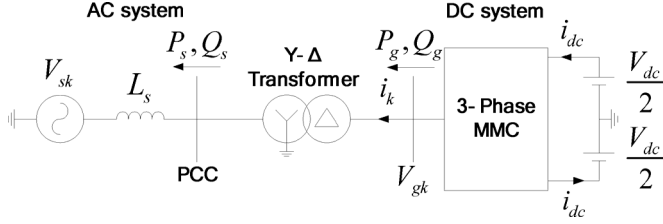positive-sequence components, negative-sequence components, zero-sequence components with double-line frequencies, and dc components. The positive-, negative-, and zero-sequence components in the instantaneous power have to be reduced because of the instantaneous power ripple. The positive- and negative-sequence components appear with a phase difference between each phase, and the zero-sequence components have the same phase in each phase. Since the zero-sequence components do not appear on a d–q axis rotational reference frame, a controller should be formed considering this. Therefore, the proposed method utilizes positive- and negative-sequence controllers in order to control positive- and negative-sequence components, respectively, in each phase and an additional zero-sequence controller to reduce the zero-sequence components. There is a disadvantage when complicating the system

in this way because notch filters and controllers are necessary to separate and control each component. Thus, the positive- and negative-sequence components were controlled through a proportional-integral-resonant (PIR) controller in a three-phase stationary frame without the need for separating the positive- and negative-sequence components. The zero-sequence components were also controlled independently through a dc-link current controller. The proposed method has the advantage of being able to control not only negative-sequence ripple, but also positive-sequence and zero-sequence ripple, under unbalanced voltage conditions. In addition, this method has the advantage of being able to improve the transient response through the direct control of dc-link currents. The effectiveness of the proposed method was verified through simulation results using PSCAD/EMTDC.

II. AC-SIDE MMC CONTROL UNDER UNBALANCED VOLTAGE

A. AC-Side Active Power Under Unbalanced Voltage

Under unbalanced voltage conditions, the active and reactive power of a grid-connected PWM converter is separated into positive- and negative-sequence components, which are expressed as shown in (1) in [21].

In (1), the total active power of a grid is represented as (2). It should be noted that the ripple with a double-line frequency was generated in the total active power, where P is the active power, Q is the reactive power, i is the grid-side current, and V is the grid-side voltage. The superscripts of p and n are positive- and negative-sequence components, respectively. Subscript g denotes the grid-side component, 0 denotes the dc component, d and q denote the d- and q-axis components in the rotational reference frame, and *sin2* and *cos2* denote the double rotational components of the line frequency, respectively

$$\begin{bmatrix} P_{g0} \\ Q_{g0} \\ P_{g\sin 2} \\ P_{g\cos 2} \end{bmatrix} = \frac{3}{2} \begin{bmatrix} V_{gd}^p & V_{gq}^p & V_{gd}^n & V_{gq}^n \\ V_{gq}^p & -V_{gd}^p & V_{gq}^n & -V_{gd}^n \\ V_{gq}^n & -V_{gd}^n & -V_{gq}^p & V_{gd}^p \\ V_{gd}^n & V_{gq}^n & V_{gd}^p & V_{gq}^p \end{bmatrix} \begin{bmatrix} i_d^p \\ i_q^p \\ i_d^n \\ i_q^n \end{bmatrix} \quad (1)$$

$$P_g = P_{g0} + P_{g\sin 2}\sin 2\omega_g t + P_{g\cos 2}\cos 2\omega_g t. \quad (2)$$

B. AC-Side Current Control

To supply active power constantly without ripple to the grid side, the ripple of the active power has to be reduced by controlling P_{gsin2} and $P_{\cos 2}$ to zero. If theta is determined such that $V_{gd}^p = 0$ through a phase-locked loop (PLL) in (1), the components of P_{gsin2} and P_{gcos2} can be expressed in terms of negative-sequence current components, as shown in (3) and (4), respectively

$$i_d^n = \frac{V_{gq}^n}{V_{gq}^p} i_d^p - \frac{V_{gd}^n}{V_{gq}^p} i_q^p \quad (3)$$

$$i_q^n = -\frac{V_{gd}^n}{V_{gq}^p} i_d^p - \frac{V_{gq}^n}{V_{gq}^p} i_q^p. \quad (4)$$
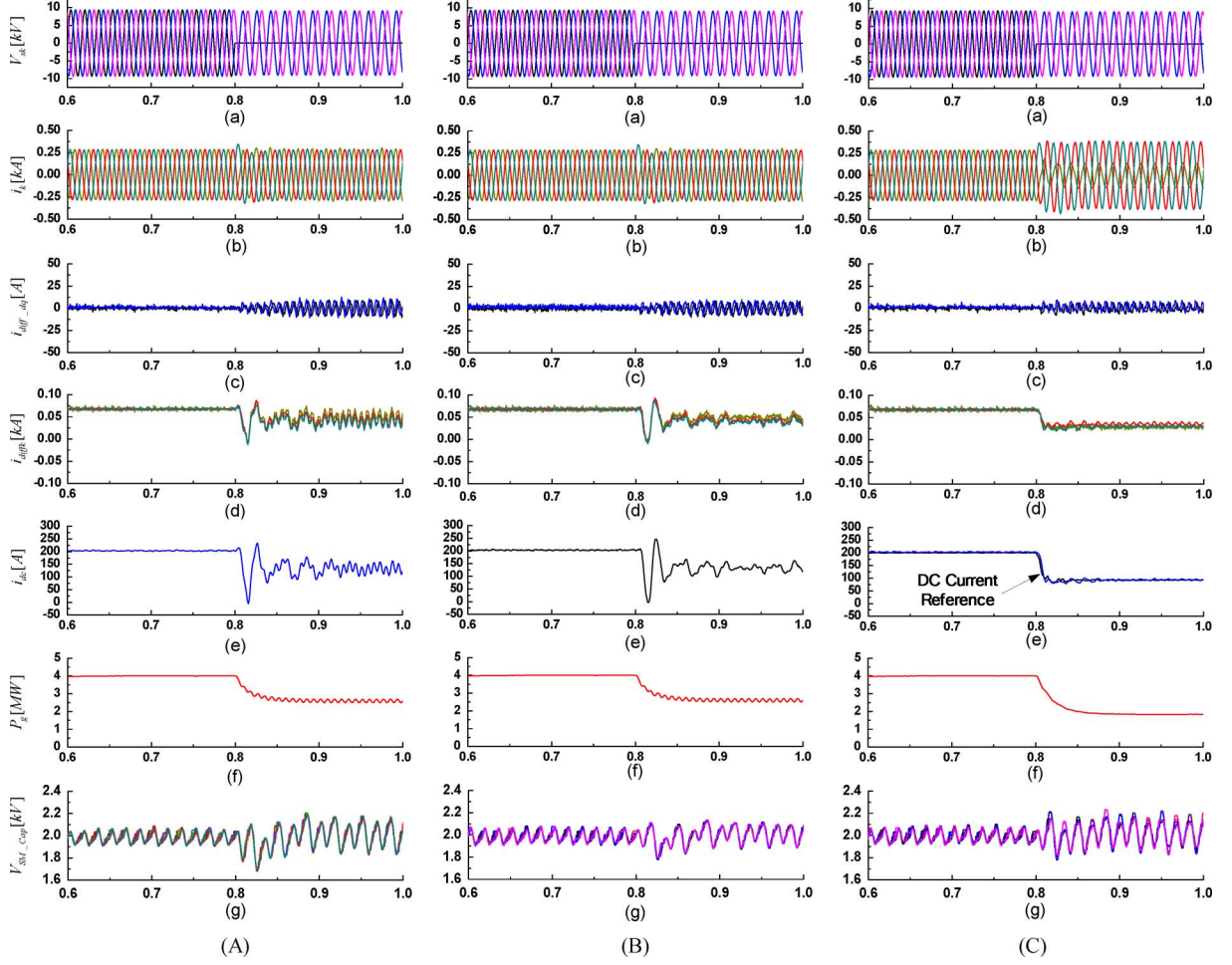
Fig. 8. MMC simulation results under the unbalanced voltage condition: (a) ac system voltage, (b) ac-side current, (c) d–q-axis circulating current, (d) inner unbalance current, (e) dc-link current, (f) grid-side active power, and (g) SM capacitor voltage. (A) Conventional method [19], (B) conventional method [2], and (C) proposed method.

The MMC's ac-side voltage equation is represented as (5) according to [19].

$$V_k = e_k - \frac{L}{2}\frac{di_k}{dt} - \frac{R}{2}i_k. \tag{5}$$

V_k is the ac-side voltage, e_k is the inner electromotive force (EMF), i_k is the ac-side current, and k denotes a, b, and c.

Since positive- and negative-sequence voltage components are generated in the grid-side voltage under unbalanced voltage conditions, (5) can be rewritten by separation into positive- and negative-sequence components as (6). V_k^p and V_k^n are ac-side positive- and negative-sequence voltages, i_k^p and i_k^n are ac-side positive- and negative-sequence currents, and e_k^p and e_k^n are positive- and negative-sequence inner electromotive forces (EMFs), respectively

$$V_k^p + V_k^n = e_k^p + e_k^n - \frac{L}{2}\frac{d}{dt}\left(i_k^p + i_k^n\right) - \frac{R}{2}\left(i_k^p + i_k^n\right). \tag{6}$$

To control the positive-sequence and negative-sequence components independently, they are separated into individual sequence components, which leads to (7) and (8) from (6)

$$V_k^p = e_k^p - \frac{L}{2}\frac{di_k^p}{dt} - \frac{R}{2}i_k^p \tag{7}$$

$$V_k^n = e_k^n - \frac{L}{2}\frac{di_k^n}{dt} - \frac{R}{2}i_k^n. \tag{8}$$

Converting (7) and (8) into a rotational reference frame, these components can be expressed as follows:

$$\frac{di_{dq}^p}{dt} = -\frac{2}{L}V_{dq}^p + \frac{2}{L}e_{dq}^p - \frac{R}{L}i_{dq}^p \mp 2\omega i_{dq}^p \tag{9}$$

$$\frac{di_{dq}^n}{dt} = -\frac{2}{L}V_{dq}^n + \frac{2}{L}e_{dq}^n - \frac{R}{L}i_{dq}^n \pm 2\omega i_{dq}^p. \tag{10}$$

If the current controllers comprise a proportional-integral (PI) controller based on (9) and (10), they can be represented as (11)

and (12). Fig. 2 shows the block diagram of the positive-sequence and negative-sequence current controllers

$$e_{dq}^{p^*} = V_{dq}^p + PI\left[i_{dq}^{p^*} - i_{dq}^p\right] \mp \omega L i_{qd}^p \tag{11}$$

$$e_{dq}^{n^*} = V_{dq}^n + PI\left[i_{dq}^{n^*} - i_{dq}^n\right] \pm \omega L i_{qd}^p \tag{12}$$

where $e_{dq}^{p^*}$ is the positive-sequence inner emf reference in the d–q axis and $e_{dq}^{n^*}$ is the negative-sequence inner emf reference in the d–q axis.

III. CIRCULATING CURRENT CONTROL

A. Phase Instantaneous Power Under Unbalanced Voltage

In an MMC, circulating currents are caused by variations in the total SM capacitor voltage in each arm. Under balanced voltage conditions, circulating currents are double-line frequency components that rotate at a negative sequence [1], [2], [19].

Fig. 3 shows a single-phase equivalent circuit in a three-phase MMC system. Here, i_{diffk} is the inner unbalance current, i_{pk} and i_{nk} are the upper and lower arms' currents, e_k is phase k's inner emf, and e_{pk} and e_{nk} are the upper and lower arm voltages, respectively.

According to Fig. 3, the MMC's voltage equation is given by [19], where V_{diffk} is the inner unbalance voltage of phase k.

$$V_{\text{diffk}} = L\frac{di_{\text{diffk}}}{dt} + Ri_{\text{diffk}} = \frac{1}{2}\left[V_{\text{dc}} - (e_{pk} + e_{nk})\right]. \tag{13}$$

The EMF is expressed as follows:

$$e_k = \frac{e_{nk} - e_{pk}}{2}. \tag{14}$$

An inner unbalance current (i_{diffk}) is expressed as (15), where $i_{\text{dc}}/3$ is the inner unbalance current's dc component, and i_{zk} is the inner unbalance current's ac component, which is the circulating current component

$$i_{\text{diffk}} = \frac{i_{pk} + i_{nk}}{2} = \frac{i_{\text{dc}}}{3} + i_{zk}. \tag{15}$$

Under unbalanced voltage conditions, the MMC's ac-side current controller injects the negative-sequence current for active power-ripple reduction. Consequently, emf contains both positive- and negative-sequence components. Thus, the MMC's upper arm voltage V_{pk} and lower arm voltage V_{nk} are expressed as (16) and (17), respectively

$$V_{pk} = \frac{V_{\text{dc}}}{2} - (e_k^p + e_k^n) - V_{\text{diffk\_ref}} \tag{16}$$

$$V_{nk} = \frac{V_{\text{dc}}}{2} + (e_k^p + e_k^n) - V_{\text{diffk\_ref}} \tag{17}$$

where $V_{\text{diffk\_ref}}$ is the compensation value of the MMC inner unbalance voltage.

In addition, the upper arm current and lower arm current are given by (18) and (19), respectively

$$i_{pk} = i_{\text{diffk}} + i_k/2 \tag{18}$$

$$i_{nk} = i_{\text{diffk}} - i_k/2. \tag{19}$$

Each phase's instantaneous power p_{PUk} is expressed as (20). p_{PUk} is defined in the Appendix, which is briefly summarized as

$$p_{PUk} = V_{pk}i_{pk} + V_{nk}i_{nk} \tag{20}$$

$$p_{PUk} = \frac{V_{\text{dc}}i_{\text{diffk}}}{2}\left[K_k^0 + K_k^{2p} + K_k^{2n} + K_k^{2z} - 2U_{\text{diffk\_ref}}\right] \tag{21}$$

where K_k^0 is the dc component, K_k^{2p} is the positive-sequence double-line frequency component, K_k^{2n} is the negative-sequence double-line frequency component, K_k^{2z} is the zero-sequence double-line frequency component, and $U_{\text{diffk\_ref}}$ is the compensation value of the MMC inner unbalanced voltage component.

Thus, each phase's instantaneous power consists not only of negative-sequence double-line frequency components, but also positive- and zero-sequence double-line frequency components. Consequently, to eliminate the instantaneous power ripple, a negative-sequence double-line frequency controller as well as positive- and zero-sequence double-line frequency controllers are necessary. The equivalent circuit is shown in Fig. 4. where $V_{PUk}^0 = V_{\text{dc}}K_k^0/2$, $V_{PUk}^{2p} = V_{\text{dc}}K_k^{2p}/2$, $V_{PUk}^{2n} = V_{\text{dc}}K_k^{2n}/2$, $V_{PUk}^{2z} = V_{\text{dc}}K_k^{2z}/2$ and $V_{\text{diffk}} = V_{\text{dc}}U_{\text{diffk\_ref}}$.

B. Circulating Current Control Under Unbalanced Voltage

In (21), K is the magnitude of the inner EMF and inner unbalanced current. The inner EMF is determined by the ac-side currents controller. Thus, to reduce the instantaneous power ripple, the inner unbalanced current ripple component should be reduced. The inner unbalance current is briefly defined

$$i_{\text{diffk}} = \frac{i_{dck}}{3} + i_{zk} = i_{dck}^0 + i_k^p + i_k^n + i_k^z \tag{22}$$

where i_k^p is the positive-sequence inner unbalanced current double-line frequency, i_k^n is the negative-sequence inner unbalance current double-line frequency, i_k^z is the zero-sequence inner unbalance current double-line frequency, i_{dck}^0 is the dc component current, and $i_{dck}^0 = i_{dck}/3, i_{zk} = i_k^p + i_k^n + i_k^z$.

The inner unbalanced current's ac component (i_{zk}) is the circulating current, which should be controlled to zero. However, to control each component like a dual vector current controller (DVCC), the notch filter and PI controller are necessary. Consequently, the controller's structure is complicated. Thus, to control each component simultaneously, a controller is constructed in a three-phase stationary frame using a PIR controller.

This has the advantage of being able to control each component without decomposition into separate components. Under balanced voltage conditions, the inner unbalanced current flowing in each phase should be controlled as $i_{\text{dc}}/3$. In addition, under unbalanced voltage conditions, the ac-side active power ripple is controlled to zero by the DVCC. This means that each phase's active power has the same magnitude. Consequently, the inner unbalanced current flowing in each phase should be controlled to $i_{\text{dc}}/3$. Thus, the circulating current controller is constructed as shown in (23). Since only the double-line frequency of the inner unbalance current's ripple

component exists, the resonant controller's cutoff frequency is set to the double-line frequency

$$V_{\text{diff\_}pn}^* = \text{PIR}[(i_{\text{dc}}/3) - i_{\text{diffk}}]. \tag{23}$$

where i_{dc} is defined as the sum of each phase's inner unbalance current. In a three-phase system, the sum of positive-sequence and negative-sequence current should be zero. Thus, idc is briefly expressed as (24), where i_{dc}^0 is $i_{\text{dca}}^0 + i_{\text{dcb}}^0 + i_{\text{dcc}}^0$ and a dc component

$$i_{\text{dc}} = i_{\text{diffa}} + i_{\text{diffb}} + i_{\text{diffc}} = (i_a^z + i_b^z + i_c^z) + i_{\text{dc}}^0. \tag{24}$$

For inner unbalanced current control, the current reference is applied to $i_{\text{dc}}/3$. Thus, the current reference includes the zero-sequence component ripple. Thus, with the PIR controller, the positive-sequence and negative-sequence component ripples can be reduced. However, the zero-sequence component ripple is not reduced. Thus, a controller to reduce this ripple component is necessary.

If it is assumed that there is no loss in the MMC, the MMC's ac-side active power P_g and dc-side active power P_{dc} should be equivalent. Under unbalanced voltage conditions, because the ac-side active power ripple is reduced through the DVCC, the ac-side active power has no ripple. The dc-side active power is given as (25). The ac-side active power and dc-link voltage are known, so the dc-link current reference is obtainable. The dc-link current reference does not contain positive, negative, nor zero sequences. Thus, the dc-link current reference can be applied to reduce the current ripples from the zero-sequence component. A controller to reduce the ripple component from the zero sequence can be constructed as shown in (27), and the control output value to control each component is defined in (28). The dc-link current controller has a characteristic that allows it to control the zero-sequence current ripple as well as providing it with a fast transient response under unbalanced voltage conditions. Fig. 5 shows a block diagram of the proposed circulating current control. It consists of three PIR controllers to control the positive- and negative-sequence circulating currents and one PIR controller to reduce the zero-sequence circulating current and dc current ripple. Fig. 6 shows a control scheme of the MMC that includes the proposed circulating current control

$$P_g = P_{\text{dc}} = V_{\text{dc}}^* i_{\text{dc}} \tag{25}$$

$$i_{\text{dc}}^* = P_g / V_{\text{dc}} \tag{26}$$

$$V_{\text{diff\_}z}^* = \text{PIR}[i_{\text{dc}}^* - i_{\text{dc}}] \tag{27}$$

$$V_{\text{diffk}}^* = V_{\text{diff\_}pn}^* + V_{\text{diff\_}z}^*. \tag{28}$$

IV. SIMULATION RESULTS

Simulation was carried out using PSCAD/EMTDC, and Fig. 7 shows the structure of the simulated system. The main circuit parameters and operating conditions are listed in Table I. The PWM method and SM's capacitor voltage-balancing algorithm uses the PSC–PWM method from [19].

Fig. 8 shows the simulation results of a conventional circulating current control method [19], a control method considering unbalanced voltage conditions [2], and the proposed circulating
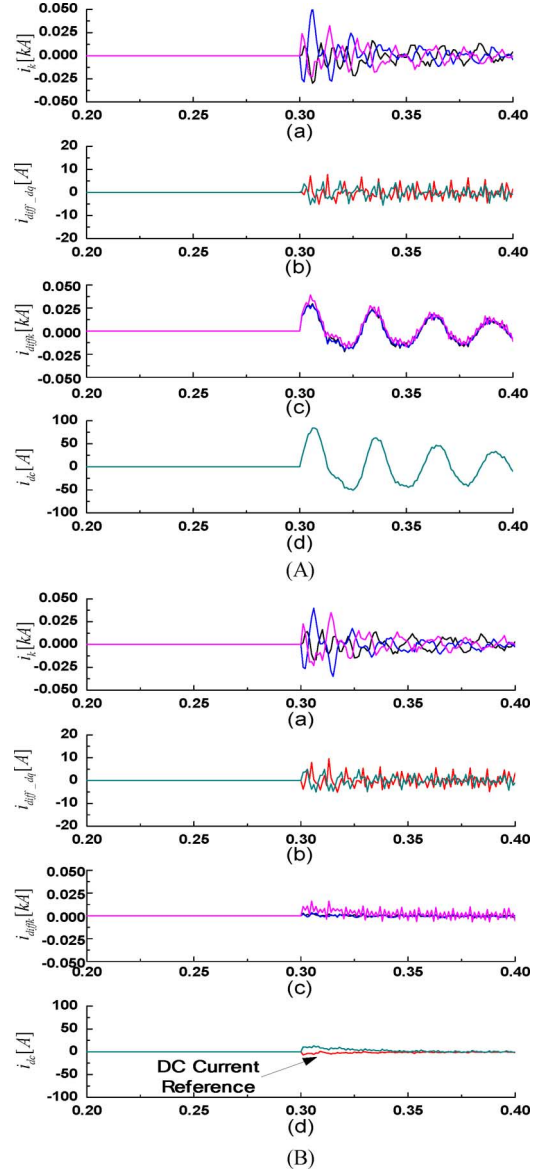

Fig. 9. MMC simulation results when PWM is applied : (a) ac-side current. (b) d–q axis circulating current, (c) inner unbalance current, (d) dc-link current. (A) Conventional method [2]. (B) Proposed method.

current control method under unbalanced voltage conditions. The ac-side positive d-axis currents reference is 0 A, and the positive q-axis currents reference is 285 A, corresponding to 4 MW at a normal voltage. The negative current references are applied according to (3) and (4). To apply unbalanced voltage conditions, the R phase line-to-ground fault is applied at 0.8 s. Fig. 8(a) and (b) shows the grid-side voltage and the MMC's ac-side currents.

Under unbalanced voltage conditions, because [19] did not consider unbalanced components, each phase's currents are controlled to a three-phase equilibrium. Furthermore, because [2] controlled the ac-side negative current to 0 A, it shows the same results as [19]. However, for the proposed control method, because the negative current is injected to reduce the active power ripple, each phase's currents are unbalanced. Fig. 8(c) shows the circulating current in a rotational reference frame. In [2] and

[19], the circulating current ripple is increased under unbalanced voltage conditions. However, the proposed control method considers components under unbalanced voltage conditions; thus, the circulating current ripple is reduced compared to that in conventional methods. However, in Fig. 8(d) and (e), each phase's inner unbalanced current and dc-link currents have severe ripple with transient currents due to ac-side active power ripple because there is an unbalanced voltage supply. Reference [19] does not control the dc-link ripple component caused by unbalanced voltage; a double-line frequency ripple is generated as well as a dc-link transient current.

Reference [2] reduced the double-line frequency ripple through a resonant controller in the dc-link component, so there is no unbalanced ripple component. However, because only a resonant controller is used, it is unable to reduce the dc-link current ripple due to the transient status. In the proposed control method, the dc-link current is directly controlled, so the dc-link current is stably controlled without transient characteristics, even through an unbalanced voltage is applied.

Fig. 8(f) shows the MMC's ac-side active power. In [2] and [19], the MMC's ac-side active power ripple cannot be reduced, so the double-line frequency ripple is generated under active power. In the proposed control method, a negative current is injected to reduce the active power ripple, so the active power ripple caused by unbalanced voltage conditions is reduced. However, the magnitude of the active power is reduced by a negative sequence's active power component. Fig. 8(g) shows the SM's capacitor voltage. The SM's capacitor voltage balancing is stably controlled because the same voltage-balancing method is used.

Fig. 9 shows the characteristics of the ac-side currents, circulating current, and dc-link current when PWM is applied. When PWM is applied, the ac-side currents are controlled at 0 A. In ac-side currents, the conventional control method and the proposed control method show similar characteristics. However, in the conventional control method, the dc-link transient current is not only controlled because of the controlling double-line frequency ripple. However, the proposed control method shows stable characteristics without ripple in the dc-link currents because the dc-link transient current is controlled when PWM is applied.

V. CONCLUSION

This paper proposed a control method for MMCs under unbalanced voltage conditions. To reduce ac-side active power ripple under unbalanced voltage conditions, ac-side components are decomposed into positive- and negative-sequence components. In addition, a DVCC is designed to control the ac-side positive and negative currents. Furthermore, the dc-side instantaneous power ripple is analyzed by ac-side positive- and negative-sequence components. Based on the analysis, a controller is designed to control the double-line frequency positive-, negative-, and zero-sequence components. The proposed control method can stably control circulating currents and the dc-link current even under unbalanced voltage conditions. In addition, the transient response is improved.

APPENDIX

The voltages of the phases of the upper arm and lower arm are given in (A1) and (A2), where $k_a^p = 2E_a^p/V_{\mathrm{dc}}, k_a^n = 2E_a^n/V_{\mathrm{dc}}, l_a^p = 2E_{\mathrm{diff\_}a}^n/V_{\mathrm{dc}}$ and α_+, α_- are the phase angles of the positive- and negative-sequence inner emfs, respectively

$$
\begin{aligned}
V_{pa} &= \frac{V_{\mathrm{dc}}}{2} - (e_a^p + e_a^n) - V_{\mathrm{diffa\_ref}} \\
&= \frac{V_{\mathrm{dc}}}{2} - \left(\begin{array}{c} E_a^p \sin(\omega_0 t + \alpha_+) \\ + E_a^n \sin(\omega_0 t + \alpha_-) \end{array} \right) - V_{\mathrm{diffa\_ref}} \\
&= \frac{V_{\mathrm{dc}}}{2} \left[1 - \left(\begin{array}{c} k_a^p \sin(\omega_0 t + \alpha_+) \\ + k_a^n \sin(\omega_0 t + \alpha_-) \end{array} \right) - U_{\mathrm{diffa\_ref}} \right]
\end{aligned}
\tag{A1}
$$

$$
\begin{aligned}
V_{na} &= \frac{V_{\mathrm{dc}}}{2} + (e_{a\_\mathrm{ref}}^p + e_{a\_\mathrm{ref}}^n) - V_{\mathrm{diffa\_ref}} \\
&= \frac{V_{\mathrm{dc}}}{2} \left[1 + \left(\begin{array}{c} k_a^p \sin(\omega_0 t + \alpha_+) \\ + k_a^n \sin(\omega_0 t + \alpha_-) \end{array} \right) - U_{\mathrm{diffa\_ref}} \right].
\end{aligned}
\tag{A2}
$$

Each arm's currents in (18) and (19) are also expressed as positive and negative sequences, respectively

$$
i_{pa} = i_{\mathrm{diffa}} \left[\begin{array}{c} 1 + m_a^p \sin(\omega_0 t + \gamma_+) \\ + m_a^n \sin(\omega_0 t + \gamma_-) \end{array} \right]
\tag{A3}
$$

$$
i_{na} = i_{\mathrm{diffa}} \left[\begin{array}{c} 1 - m_a^p \sin(\omega_0 t + \gamma_+) \\ - m_a^n \sin(\omega_0 t + \gamma_-) \end{array} \right]
\tag{A4}
$$

where m_a^p is the positive-sequence current modulation index, m_a^n is the negative-sequence modulation index, and γ_+ and γ_- are the positive- and negative-phase angles of the converter ac output current, respectively.

Substituting (A1)–(A4) into (20), each phase's instantaneous power is given as

$$
p_{PUk} = \frac{V_{\mathrm{dc}} i_{\mathrm{diffk}}}{2} \left[\begin{array}{c} \mathrm{Item1}_k + \mathrm{Item2}_k \\ + \mathrm{Item3}_k + \mathrm{Item4}_k \end{array} \right]
\tag{A5}
$$

where

$$
\begin{aligned}
\mathrm{Item1}_a &= 2 - 2U_{\mathrm{diffa\_ref}} - k_a^p m_a^p \cos(\alpha_+ - \gamma_+) \\
&\quad - k_a^n m_a^p \cos(\alpha_- - \gamma_+) - k_a^n m_a^n \cos(\alpha_+ - \gamma_-) \\
&\quad - k_a^n m_a^n \cos(\alpha_- - \gamma_-) \\
\mathrm{Item2}_a &= k_a^p m_a^p \cos(2\omega_0 t + \alpha_+ + \gamma_+) \\
\mathrm{Item3}_a &= k_a^n m_a^n \cos(2\omega_0 t + \alpha_- + \gamma_-) \\
\mathrm{Item4}_a &= k_a^n m_a^p \cos(2\omega_0 t + \alpha_- + \gamma_+) \\
&\quad + k_a^p m_a^n \cos(2\omega_0 t + \alpha_+ + \gamma_-).
\end{aligned}
$$

Equation (A5) is separated into individual components and defined as follows:

Item 1) dc component and regulating the unbalanced voltage;
Item 2) double-line frequency negative sequence;
Item 3) double-line frequency positive sequence;
Item 4) double-line frequency zero sequence.

Thus, under unbalanced voltage conditions, to reduce the ac-side active power ripple from the MMC, if there is a negative-sequence component in the ac side, each phase's power does not have only the dc component and the negative-sequence

double-line frequency component, but also positive-sequence and zero-sequence double-line frequency components.

Here, because the positive sequence, negative sequence, and zero sequence are active power-ripple components, they should be controlled to 0 through $U_{\mathrm{diffk\_ref}}$.

References

[1] A. Antonopoulos, L. Angquist, and H. P. Nee, "On dynamics and voltage control of the modular multilevel converter," in *Proc. Eur. Conf. Power Electron. Appl.*, Barcelona, Spain, 2009, pp. 1–10.

[2] Q. Tu, Z. Xu, Y. Chang, and L. Guan, "Suppressing DC voltage ripples of MMC-HVDC under unbalanced grid conditions," *IEEE Trans. Power Del.*, vol. 27, no. 3, pp. 1332–1338, Jul. 2012.

[3] N. Flourentzou, V. G. Agelidis, and G. D. Demetriades, "VSC-based HVDC power transmission systems: An overview," *IEEE Trans. Power Electron.*, vol. 24, no. 3, pp. 592–602, Mar. 2009.

[4] Y. H. Liu, J. Arrillaga, and N. R. Watson, "Cascaded H-bridge voltage reinjection—Part I: A new concept in multilevel voltage-source conversion," *IEEE Trans. Power Del.*, vol. 23, no. 2, pp. 1175–1182, Apr. 2008.

[5] Q. Tu and Z. Xu, "Impact of sampling frequency on harmonic distortion for modular multilevel converter," *IEEE Trans. Power Del.*, vol. 26, no. 1, pp. 298–306, Jan. 2011.

[6] J. Qin and M. Saeedifard, "Predictive control of a modular multilevel converter for a back-to-back HVDC system," *IEEE Trans. Power Del.*, vol. 27, no. 3, pp. 1538–1547, Jul. 2012.

[7] B. Andersen, L. Xu, P. J. Horton, and P. Cartwright, "Topologies for VSC transmission," *Power Eng. J.*, vol. 16, no. 3, pp. 142–150, Jun. 2002.

[8] M. Saeedifard, R. Iravani, and J. Pou, "A space vector modulation strategy for a back-to-back five-level HVDC converter system," *IEEE Trans. Ind. Electron.*, vol. 56, no. 2, pp. 452–466, Feb. 2009.

[9] S. Li, T. Haskew, and L. Xu, "Control of HVDC light system using conventional and direct current vector control approaches," *IEEE Trans. Power Electron.*, vol. 25, no. 12, pp. 3106–3118, Dec. 2010.

[10] A. Lesnicar and R. Marquardt, "A new modular voltage source inverter topology," presented at the 10th Eur. Conf. Power Electron. Appl., Toulouse, France, 2003.

[11] M. Saeedifard and R. Iravani, "Dynamic performance of a modular multilevel back-to-back HVDC system," *IEEE Trans. Power Del.*, vol. 25, no. 4, pp. 2903–2912, Oct. 2010.

[12] S. Rohner, S. Bernet, M. Hiller, and R. Sommer, "Modelling, simulation and analysis of a modular multilevel converter for medium voltage applications," in *Proc. IEEE Int. Conf. Ind. Technol.*, Vina del Mar, Chile, 2010, pp. 775–782.

[13] U. Gnanarathna, A. Gole, and R. Jayasinghe, "Efficient modeling of modular multilevel HVDC converters (MMC) on electromagnetic transient simulation programs," *IEEE Trans. Power Del.*, vol. 26, no. 1, pp. 316–324, Jan. 2011.

[14] H. Huang, "Multilevel voltage-sourced converters for HVDC and FACTs applications," presented at the CIGRÉ Conf., Bergen and Ullensvang, Norway, 2009.

[15] J. Dorn, H. Huang, and D. Retzmann, "A new multilevel voltage-sourced converter topology for HVDC applications," presented at the CIGRE Session, B4-304, Paris, France, 2008.

[16] R. Marquardt, "Stromrichterschaltungen mit Verteilten Energiespeichern," German Patent DE10103031A1, Jan. 24, 2001.

[17] Q. Tu, Z. Xu, H. Huang, and J. Zhang, "Parameter design principle of the arm inductor in modular multilevel converter based HVDC," in *Proc. Int. Conf. Power Syst. Technol.*, Hangzhou, China, 2010, pp. 1–6.

[18] A. Lesnicar, "Neuartiger, modularer mehrpunktumrichter M2C für netzkupplungsanwendungen," Ph.D. dissertation, Dept. Elect. Eng. Inf. Technol., Univ. Bundeswehr, Munich, Germany, 2008.

[19] Q. Tu, Z. Xu, and L. Xu, "Reduced switching-frequency modulation and circulating current suppression for modular multilevel converters," *IEEE Trans. Power Del.*, vol. 26, no. 3, pp. 2009–2017, Jul. 2011.

[20] Z. Yuebin, J. Daozhuo, G. Jie, H. Pengfei, and L. Zhiyong, "Control of modular multilevel converter based on stationary frame under unbalanced AC system," in *Proc. 3rd Int. Conf. ICDMA*, 2012, pp. 293–296.

[21] L. Xu and Y. Wang, "Dynamic modeling and control of DFIG based wind turbines under unbalanced network conditions," *IEEE Trans. Power Syst.*, vol. 22, no. 1, pp. 314–323, Feb. 2007.

Ji-Woo Moon (S'13) was born in Pusan, Korea, in February 1981. He received the B.S. and M.S. degrees in electrical engineering from Dong-A University, Pusan, Korea, in 2006 and 2008, respectively, where he is currently pursuing the Ph.D. degree in electrical engineering at Pusan National University, Pusan.

Since 2008, he has been with Korea Electrotechnology Research Institute, Changwon, Korea. His present interests include control of HVDC, wind energy generation, and the application of power electronics to power systems.

Chun-Sung Kim (S'13) was born in Kwang-Ju, Koera, on August 22, 1982. He received the M.S. degrees in electrical engineering from Chunnam National University, Kwang-ju, Korea, in 2011, where he is currently pursuing the Ph.D. degree at Chunnam National University, Kwang-ju, Korea.

He has been with Korea Electrotechnology Research Institute, Chang-won, Korea, since 2012. His research nterests are control of HVDC, wind energy generation, and the application of power electronics to power systems.

Jung-Woo Park was born in Chungnam, Korea, in February 1963. He received the B.S. and M.S. degrees in electronic engineering from Chungnam National University, Chungnam, Korea, in 1986 and 1988, respectively, and the Ph.D. degree in electrical engineering from Kyungpook National University, Kyungpook, Korea.

Since 1998, he has been a Principal Researcher with the Korea Electrotechnology Research Institute, Changwon, Korea. His research interests include control of HVDC, multilevel converter, wind energy generation, and renewable energy.

Dae-Wook Kang (S'99–M'04) received the B.S., M.S., and Ph.D. degrees in electrical engineering from Hanyang University, Seoul, Korea, in 1998, 2000, and 2004, respectively.

Since 2004, he has been with the Korea Electrotechnology Research Institute, Changwon, Korea, as a Senior Researcher. His present interests include the control of HVDC, multilevel converters, renewable energy, and the application of power electronics to power systems.
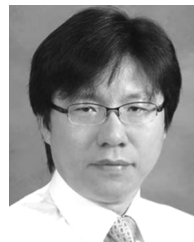
Jang-Mok Kim (M'01) was born in Pusan, Korea, in August 1961. He received the B.S. degree in electrical engineering from the Pusan National University (PNU), Pusan, in 1988, and the M.S. and Ph.D. degrees from in electrical engineering from Seoul National University, Seoul, Korea, in 1991 and 1996, respectively.

From 1997 to 2000, he was a Senior Research Engineer at the Korean Electric Power Research Institute (KEPRI). Since 2001, he has been with the School of Electrical Engineering, PNU, where he is currently a Faculty Member and a Research Member of the Research Institute of Computer Information and Communication. As a Visiting Scholar, he joined the Center for Advanced Power Systems (CAPS), Florida State University, Tallahassee, FL, USA. His research interests include control of electric machines, electric-vehicle propulsion, and power quality.